# Design and 3D printing of a modular phantom of a uterus for medical device validation

*Sara Candidori, Serena Graziosi and Paola Russo*
Department of Mechanical Engineering, Politecnico di Milano, Milan, Italy

*Kasra Osouli and Francesco De Gaetano*
Department of Chemistry, Materials and Chemical Engineering "G. Natta", Politecnico di Milano, Milan, Italy

*Alberto Antonio Zanini*
Obstetrician Gynecologist, Milan, Italy, and

*Maria Laura Costantino*
Department of Chemistry, Materials and Chemical Engineering "G. Natta", Politecnico di Milano, Milan, Italy

## Abstract

**Purpose** – The purpose of this study is to describe the design and validation of a three-dimensional (3D)-printed phantom of a uterus to support the development of uterine balloon tamponade devices conceived to stop post-partum haemorrhages (PPHs).

**Design/methodology/approach** – The phantom 3D model is generated by analysing the main requirements for validating uterine balloon tamponade devices. A modular approach is implemented to guarantee that the phantom allows testing these devices under multiple working conditions. Once finalised the design, the phantom effectiveness is validated experimentally.

**Findings** – The modular phantom allows performing the required measurements for testing the performance of devices designed to stop PPH.

**Social implications** – PPH is the leading obstetric cause of maternal death worldwide, mainly in low- and middle-income countries. The proposed phantom could speed up and optimise the design and validation of devices for PPH treatment, reducing the maternal mortality ratio.

**Originality/value** – To the best of the authors' knowledge, the 3D-printed phantom represents the first example of a modular, flexible and transparent uterus model. It can be used to validate and perform usability tests of medical devices.

**Keywords** 3D printing, Design for additive manufacturing, Phantom, Device validation, Post-partum haemorrhage

**Paper type** Research paper

## 1. Introduction

Physical models of organs, or phantoms, are already used in medicine to plan and simulate surgical operations, develop and test new devices and train medical staff and patients. Additive manufacturing (AM), coupled with tomographic scans of the human body, makes it possible to obtain highly accurate and patient-specific, three-dimensional (3D) physical models at a relatively contained cost. Through these models, surgeons can select the most suitable surgical approach and estimate surgical risks in the preoperative stage without using cadaveric samples, avoiding the transmission of infectious agents and solving ethical issues (Wang *et al.*, 2017). Despite this broad use of 3D-printed phantoms, their application in the field of the reproductive system and, more generally, in gynaecology is still limited (Flaxman *et al.*, 2021), even if a few interesting examples are already available (Cooke *et al.*, 2019; Flaxman *et al.*, 2021; Kondoh *et al.*, 2019; Mackey *et al.*, 2019; Sayed Aluwee *et al.*, 2017). This is a relevant issue because phantom could be used to assist reproductive techniques, help presurgical planning, provide additional support for validating medical devices and favour studies on endometriosis (Barbosa *et al.*, 2019). Indeed, several gynaecological simulators are already available on the market, but they are, for example, not conceived for *validating* medical devices. This study is part of a broader project focused on developing an innovative device for treating an obstetric emergency called post-partum

haemorrhage (PPH). Thanks to 3D-printing technology, the study aims to address the lack of a proper validation setup and related procedure to drive the preliminary lab testing of this device as a fundamental step for supporting its development.

PPH is defined as blood loss above 500 ml within 24 h of birth. It is the leading obstetric cause of maternal mortality worldwide, especially in low- *and* middle-income countries (LMICs) (World Health Organization, 2012). Reducing the global maternal mortality ratio is one of the targets of the third Sustainable Development Goal (SDG 3, Good health and well-being) of the United Nations (United Nations, 2021). The most common cause of PPH is uterine atony. The myometrial contraction that follows delivery is the first mechanism of haemostasis, and when uterine tissue loses tone, bleeding occurs. PPH can be managed in developed countries using uterotonic drugs and uterine balloon tamponade (UBT) devices like the Bakri® Postpartum balloon, consisting of a double-lumen catheter that allows blood drainage and monitoring of the bleeding (Cook Medical, 2021).

On the contrary, PPH is life-threatening in LMICs, because UBT solutions are prohibitive due to their costs. The low-cost alternative to UBT is the so-called "condom balloon tamponade" (CBT) solution (World Health Organization, 2012). This solution consists of a condom tied to a catheter through strings, inserted into the uterus through the cervix and filled with physiological solution or water to stop the bleeding (Figure 1). However, the methods used to connect the condom to the catheter usually result in leakage, and specific training is required to perform the procedure. Attempts to overcome these limitations are available (Massachusetts General Hospital, 2021; Mishra *et al.*, 2016) with few results. Therefore, developing a new low-cost CBT kit for LMICs is necessary.

The mechanism of action of UBT devices in stopping the bleeding is a combination of several concurring factors (Georgiou, 2012). However, if the balloon's pressure on the uterine wall is higher than that of the bleeding vessel, then the bleeding should stop (Condous *et al.*, 2003; Danso and Reginald, 2012). In years, the effectiveness of UBT devices was also observed *in-vivo* using devices working at lower pressures (Antony *et al.*, 2017; Belfort *et al.*, 2011; Georgiou, 2010; Kong and To, 2018). Nowadays, new UBT solutions should demonstrate their equivalence to devices already on the market for being commercialised as medical devices, following the Food and Drug Administration (FDA) premarket notification or the 510(k) pathway (Food and Drug Administration, 2021). Multiple tests are usually performed to assess the mechanical properties of these devices, including, for example, the measurement of the intraluminal pressure (ILP), that is, the

pressure inside the balloon/condom, and of the intrauterine pressure (IUP), that is, the pressure exerted by the balloon/condom on the internal uterine walls. However, how to perform these measurements, i.e. the procedure to follow and the necessary testing setup, is not specified.

In this study, the testing setup described in Mollazadeh-Moghaddam *et al.* (2019) was considered a reference because it was used to test a CBT device that received FDA approval (Food and Drug Administration, 2019).

Then, we exploited the potential of AM technologies to provide an effective strategy to improve and make systematic the design and validation phases of new CBT solutions. To this aim, we developed a modular 3D-printed phantom of the woman's uterus (where the PPH occurs and the UBT/CBT device is inserted), whose effectiveness was validated by testing a commercial CBT device. The uterus phantom allows usability testing, as CBT solutions require specific training about their assembly and correct usage. Hence, the contribution of this paper is to demonstrate the potential of 3D-printed phantoms in supporting the design and testing of a gynaecological medical device.

The paper is organised as follows: Section 2 presents the state-of-the-art in the use of anatomical 3D-printed phantoms in medicine, with a focus on the gynaecological field; Section 3 describes the method used to design and 3D-print the proposed modular phantom and the protocols of the validation tests; Section 4 presents the obtained results; in Section 5, conclusions are reported.

## 2. Background

Although virtual models and technologies are increasing in the medical field, physical models provide tactile feedback and a better perception of the dimensions of the organ, thus allowing surgeons to develop a clearer understanding of the surgical anatomy (Marconi *et al.*, 2017; Smelt *et al.*, 2019). Unlike conventional manufacturing methods, AM technologies have made more affordable the possibility to create high-quality phantoms (Gebhardt, 2012), especially for visual inspections in several surgical subspecialties such as cardiac surgery (Bartel *et al.*, 2018; Giannopoulos, Mitsouras, *et al.*, 2016; Giannopoulos, Steigner, *et al.*, 2016; Kim *et al.*, 2008; Riedle *et al.*, 2021; Vukicevic *et al.*, 2017; Yoo *et al.*, 2016; Yoo and van Arsdell, 2018), neurosurgery (Baskaran *et al.*, 2016; Randazzo *et al.*, 2016; Vakharia *et al.*, 2016), spine surgery (Garg and Mehta, 2018; Senkoylu *et al.*, 2020; Sheha *et al.*, 2019; Wilcox *et al.*, 2017), craniomaxillofacial surgery (Choi and Kim, 2015; Ghai *et al.*, 2018; Meglioli *et al.*, 2020), abdominal surgery (Bangeas *et al.*, 2019; Muguruza Blanco *et al.*, 2019; Perica and Sun, 2018; Pietrabissa *et al.*, 2020; Soon *et al.*, 2016; Sun, 2020; Tejo-Otero *et al.*, 2021; Witowski *et al.*, 2017), thoracic surgery (Giannopoulos, Steigner, *et al.*, 2016) and urology (Ghazi and Teplitz, 2020; Mathews *et al.*, 2020). In preoperative planning, these models allow surgeons to visualise the patient's anatomy, anticipate potential difficulties and tailor their surgical approach accordingly. Physical models help reduce intraoperative time, minimise anaesthetic and radiation dosage and optimise surgical outcomes. If the phantom can replicate the consistency of biological tissues, then it may also allow the simulation of the operation.

**Figure 1** How a condom balloon tamponade kit works: (a) the deflated probe cover; (b) the inflated probe cover. Images inspired by (MedicalAidFilms, 2021; Candidori *et al.*, 2021)
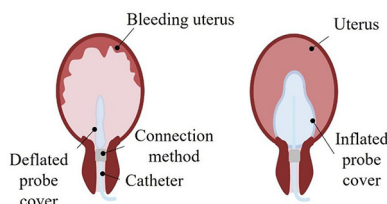
However, to provide 3D-printed phantoms which such a capability, further research efforts are needed because of the difficulties of correctly mimicking the behaviour, particularly of soft living tissues, with currently available materials (Tejo-Otero *et al.*, 2022; Tejo-Otero *et al.*, 2020a; Tejo-Otero *et al.*, 2020b).

3D-printed phantoms can enhance the education of trainees and patients and can be used to facilitate interdisciplinary communication between health-care providers (Yap *et al.*, 2017). Current surgical training in several specialities is mostly opportunity-based, limiting the trainees' constant exposure to the various procedures. However, most of the existing simulators used for educational purposes only roughly mimic the details of human organs' morphology and physical properties. The preoperative visual inspections can potentially revolutionise surgical education, leading to a requirement-based standardised approach (Giannopoulos, Mitsouras, *et al.*, 2016). Besides, 3D-printed models represent an effective and innovative tool at the disposal of the specialist and the patient, capable of bridging the language gap between these figures through a practical and tangible approach. They also increase the awareness of the patients and their families regarding the risk of the operation and make it easier for the surgeon to obtain informed consent (Marone *et al.*, 2018). Eventually, anthropomorphic 3D-printed models are increasingly used to validate and test medical devices because they allow for preliminary validation before running *in-vivo* experiments.

As already underlined, a few examples of phantoms for surgical treatment of gynaecological pathologies exist in the literature. In Ajao *et al.* (2017), a 3D-printed model of deep infiltrating endometriosis with an unusual nodules' location was generated from magnetic resonance imaging (MRI) to support the selection of the best surgical approach for the specific case study. In Flaxman *et al.* (2021), 3D-printed patient-specific models were obtained from MRI-derived images for surgical planning and risk reduction of complex myomectomies, that is, removal of uterine fibroids. Anthropomorphic phantoms were also used for preoperative evaluation of complex hysterectomies, that is, the uterus' removal. In Sayed Aluwee *et al.* (2017), two technologies were combined to obtain five patient-specific polymeric uterus phantoms to improve the accuracy of the surgical procedure. In Mackey *et al.* (2019), an extrusion-based technology is used to obtain a patient-specific uterine model and highlight the best location to apply the incision for a complex caesarean delivery because of fibroids. In Kondoh *et al.* (2019), a postpartum uterine cavity model was manufactured using stereolithography, starting from computed tomography (CT) data. However, the authors themselves highlighted as limitations the fact that the model was derived from CT images of a single patient and that it barely mimics the elastic properties of the tissue. Eventually, in Cooke *et al.* (2019), two cases of 3D-printed patient-specific models for the preoperative planning of minimally invasive gynecologic surgeries are presented. They are created by following a dedicated protocol and using MRI.

Gynaecological and obstetric training is primarily performed using simulators, commercial products conceived only for the education of healthcare providers (Laerdal, 2021a; Limbs and Things, 2021). Medical professionals use uterus simulators for exercises involving the simulation of vaginal deliveries and possible bleeding, significantly reducing severe haemorrhage cases and blood transfusion rates after birth (DeStephano *et al.*, 2015). However, while commercial simulators are suitable for training, they cannot be used for device validation.

These models are often unrealistic and loosely reflect the specific morphological characteristics of the tissues but only replicate the dimensions of the female uterus. Being not transparent, they do not allow us to visualise the inside of the organ. The data in the literature regarding the characterisation of uterine or cervical tissue refer primarily to tests performed on pathological tissues obtained following hysterectomies. These data do not provide helpful information regarding the change in the mechanical behaviour of the tissue during the various stages of pregnancy and childbirth and refer to specific portions of the organ. One of the few studies available in the literature to deal with this lack is Myers *et al.* (2010). In this paper, a mechanical testing protocol was developed to investigate the response of pathological cervical tissue to uniaxial tension and compression. Mechanical responses were compared between samples obtained through hysterectomies in patients with different obstetric backgrounds. The results demonstrate the anisotropy of the cervical tissue, the asymmetry between the two studied loading conditions and the dependence of mechanical properties on obstetrical experience. Two further studies (Kauer *et al.*, 2002; Mazza *et al.*, 2006) describe the mechanical properties of the human uterine cervix and body evaluated through *in-vivo* and *ex-vivo* aspiration experiments. Tests were performed by inserting an aspiration device, consisting of a tube in which the internal pressure can be controlled, into the organ. By pushing it against the tissue and creating a vacuum, the tissue is sucked through the aspiration area: images of the tissue profile are simultaneously acquired and analysed. However, these data help compare patients with different pathologies. Eventually, indentation tests are performed on uterine tissue samples excised from several anatomical locations (fundus, anterior and posterior wall of the uterus) and sliced through their thickness (Fang *et al.*, 2021). The results show that the uterine tissue displays heterogeneous and anisotropic mechanical properties at different locations and across different layers through the wall. Again, however, the pathological nature of the specimens influences the results. Despite all these relevant efforts, the lack of data on the characterisation of healthy uterine and cervical tissues makes it challenging to develop a uterine phantom with mechanical characteristics similar to the physiological organ during and after pregnancy.

However, despite this lack of data, given the relevance of developing an adequate setup for testing gynaecological devices, there are few cases regarding developing reproductive system phantoms for device validation in the literature. In Whalen *et al.* (2021), a cervical phantom, not 3D-printed, was designed to simulate the compressive force exerted by the cervix on a mechanical device to achieve optimal dilation during delivery. This physical model made it possible to verify that the device enables vaginal delivery by preventing retraction of the cervix against the foetus during delivery.

In Mollazadeh-Moghaddam *et al.* (2019), three machined aluminium uterus phantoms of three different sizes were made to test CBT devices and evaluate their function when subjected

to high ILP values. The proposed aluminium phantom does not allow seeing inside the cavity, and its rigidity does not simulate uterine and cervical tissue consistency. A further study (Hu *et al.*, 2020) proposed a phantom of a uterus in three different sizes. They were 3D-printed in polycaprolactone to validate a UBT device. In this case, the phantoms were designed to measure the IUP value, that is, the pressure exerted by the balloon on the uterine walls. Also, in this case, the uterine models are rigid and unable to mimic the elastic and contractile properties of the uterine muscle. In addition, the different sizes of the models represent the different sizes that the uterus reaches during gestation but do not mimic the variable dilations of the cervix. This phantom only represents the uterus and fails to mimic the vagina, as it lacks tissue at the cervical end of the uterine model. The authors underlined this proved to be a problem: the device occasionally expands slightly outside the model through the cervical opening, affecting the intrauterine pressure exerted by the balloon on the phantom walls.

As highlighted through this state-of-the-art analysis, there is the need to design and fabricate a phantom of a uterus that could work as an effective setup for UBT/CBT devices' validation and approval because current commercial simulators are not designed for this purpose. To address this need, we propose a method for designing and fabricating a modular uterine phantom that overcomes the limitations of commercial simulators and existing phantoms for medical device validation.

## 3. Materials and methods

### 3.1 Definition of the phantom design requirements

Before starting the design of the modular phantom, an analysis of the structure of the real organ was made. This analysis is essential to evaluate the biomechanical characteristics of each part of the organ and tissue relevant for validating a UBT/CBT device. Besides, it was also crucial to reach a proper trade-off between the effectiveness of the phantom for the device testing and the need to guarantee its technical feasibility.

The uterus or uterine cavity is composed mainly of two portions that have different physiological functions and mechanical behaviour: the body of the uterus and the cervix. The literature is confusing, as the term uterine cavity is used to describe the endometrial cavity with the endocervical canal by some authors and the endometrial cavity only by others (Goldstuck, 2012). In this paper, the term *uterine cavity* represents the inner of the uterus without the endocervical canal and opening. During the labour, the cervix dilates, and PPH could occur immediately after the delivery or some hours later (within 24 h). PPH could also arise after caesarean delivery: in this case, there could be different cervix dilation conditions according to what time of labour or even out of childbirth the caesarean section takes place. From these initial considerations, the requirements for the design of the phantom were set.

The first requirement is to reproduce the actual size and shape of the uterus at the time of delivery. Data were taken from a study on two-dimensional ultrasound images of the uterus and cervix in pregnant subjects (Louwagie *et al.*, 2021). However, it is worth pointing out that during pregnancy, the uterine tissue easily adapts to the size of the foetus and can

quickly recover its size after delivery, thanks to the contraction process that follows the birth. Because of the loss of tissue tone, which can occur in some clinical cases, the uterus cannot contract after delivery. This is one of the main complications leading to PPH. UBT or CBT devices allow to tamponade the tissue and stop bleeding; they should stay inside the uterus for 24 h. Hence, it is essential to test them in a phantom reproducing the uterus' size at the delivery time. The uterus phantom described in Edwards and Ellwood (2000) roughly mimics the size and shape of the organ a few days or a week after delivery. However, it is also correct to consider the uterus' tissue as atonic and, therefore, unable to contract. In such a situation, the organ does not quickly reduce in size.

A second requirement related to the previous one is to validate the device in its worst working conditions in terms of maximum and minimum cervix dilations. Hence, developing a phantom that simulates the adaptations of the single parts throughout the gestation period and finally with delivery is necessary. In addition, cervical dilations and the different inclinations of the uterine walls, which change according to the dilation size, need to be considered.

Given the necessity to validate a UBT device, the phantom should allow the measurement of all the required parameters (i.e. the ILP and IUP values). At the same time, for performing usability tests, the possibility of simulating the bleeding should be implemented. As we are dealing with a bleeding process and, thus, with a fluid, the phantom should also guarantee hydraulic sealing.

Data related to uterine tissue samples obtained from hysterectomies (Myers *et al.*, 2008) were also considered to choose the most appropriate material to reproduce the flexibility of the uterine walls. An additional requirement related to the material selection was the phantom's transparency. This characteristic allows for checking the inside of the organ during the inflation procedure of the device.

All these requirements were matched with the necessity to guarantee the printability of the designed phantom using state-of-the-art 3D printing machines and materials to quickly validate its effectiveness and foster a wide diffusion of the proposed solution.

A summary of the requirements is reported in Table 1. The three main design needs from which they were derived are the anatomical conformation of the phantom, the possibility of performing all the necessary validation tests of the device and the technical feasibility of the phantom.

### 3.2 Design of the phantom

A modular solution was considered to simulate the different dilations that can occur after delivery. The phantom was designed as a single uterus body coupled with different cervices. The uterine body was designed by referring to data taken from two studies. In Louwagie *et al.* (2021), several measurements of the structural dimensions of the gravid uterus and cervix during gestation are available, while in Paliulyte *et al.* (2017), fewer parameters (uterine size in the three directions) are provided. The phantom was created using Autodesk Inventor®. In Figure 2(a), its exploded view is shown. It consists of the uterus body, three interchangeable cervices, two flanges and a sealing ring. Three cervix models with different distal diameters and extensions were considered to simulate diverse delivery

**Table 1** Definition of the phantom primary design needs and requirements

| Requirements | Adequate anatomical conformation of the phantom | Needs<br>Possibility to perform all the necessary validation tests of the device | Technical feasibility of the phantom |
|---|:---:|:---:|:---:|
| The anatomical shape/size of the phantom must mimic the uterus at the time of the delivery | ✓ | ✓ | |
| The phantom must allow the testing of the device in different delivery conditions | ✓ | ✓ | |
| The ILP and IUP values must be measurable | | ✓ | |
| The phantom must simulate the flexibility of the uterine walls | ✓ | ✓ | |
| The phantom must allow the visual monitoring of the inflation process of the condom/balloon | | ✓ | |
| The phantom should be printable using state-of-the-art 3D printing machines and materials | | | ✓ |

**Figure 2** CAD model of the uterus phantom: (a) exploded view; (b) the assembled CAD model with the 20 mm cervix, (c) with the 50 mm cervix and (d) with the 80 mm cervix. The "extension" and "diameter" dimensions correspond to the values reported in Table 2
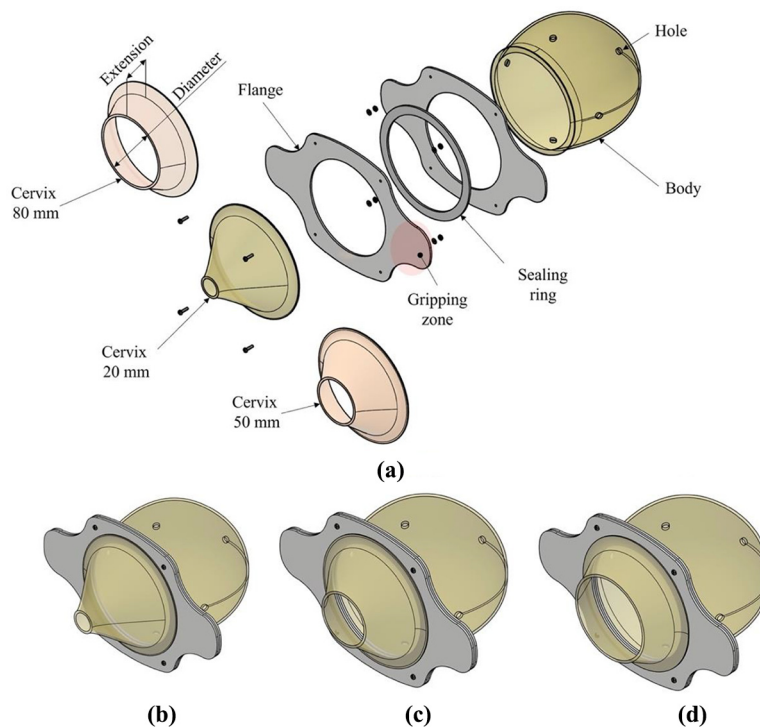


conditions. The three distal diameters are 20 mm, 50 mm and 80 mm, corresponding to three situations during which PPH could occur. The assembled versions are shown in Figures 2(b)–(d). The uterus body has five holes [Figure 2(a)] that were modelled to allow the connection of pressure transducers to measure the IUP. The extremities of the flanges were designed as gripping areas for the phantom to allow different modalities for orienting the uterus body. The phantom's orientations with respect to the horizontal plane (i.e. 100°, 90° and 80°) were estimated and set based on a discussion with the gynaecologist. A reclinable structure was also modelled to precisely control the phantom

orientation and guarantee a stable positioning during the simulation of the device insertion [Figure 3(a)].

An elliptical shape with a vertical semi-axis of 50 mm and a horizontal semi-axis of 55 mm was used to create the internal sections of the uterus in the posterior part. For the anterior part of the uterus, in contact with the plane of separation with the cervix, a circular shape with a 110 mm diameter was used [Figure 3(b)]. The values in Table 2 were used to model the three cervixes [Figures 2(b)–(d)]. The internal volume of the phantom's cavity is between 2.5 l and 3 l in the three configurations.

**Figure 3** (a) CAD model of the uterus phantom and the reclinable support; and (b) CAD model of the uterus and cervix structure with main dimensions



(a)

(b)
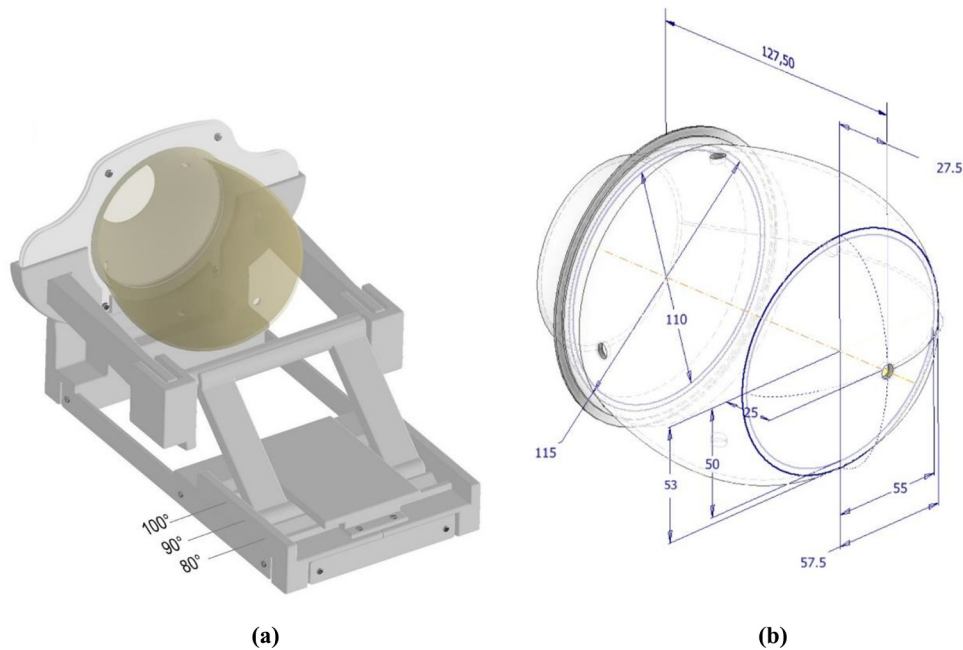
**Table 2** Dimensions of the three different cervixes with diameters of 20, 50 and 80 mm (Figure 2)

| Cervix model | Diameter [mm] | Extension [mm] |
|---|---|---|
| 1 | 20 | 65.5 |
| 2 | 50 | 40 |
| 3 | 80 | 33 |

For prototyping the phantom, the Formlabs Flexible 80 A resin (Formlabs Inc., 2017) was used together with the Form 3B printer (Formlabs Inc.). This resin has a Shore Hardness equal to 80 A and is semi-transparent. Tensile tests were performed on three dog-bone specimens vertically 3D-printed with the selected resin and sized according to ASTM D412 (ASTM International, 2021) to characterise the material. The manufacturer's indications for this material were followed to cure the resin (i.e. 10 min at 60°C). The machine used for the tensile tests is the MTS Alliance RT/10 equipped with a 1 kN load cell. Tests were performed under displacement control using a crosshead speed of 500 mm/min and data acquisition at 20 Hz. A tensile modulus of 17 MPa was obtained.

Because of the limited data in the literature regarding the characterisation of healthy and living uterine tissue, seven specimens with a rectangular cross-section (10 mm × 30 mm) and a height/thickness ranging from 2 to 8 mm, respectively, were 3D-printed. A gynaecological surgeon with over 30 years of clinical and surgical experience was asked to interact with them manually and to identify the sample with a consistency closer to that of uterine walls. Based on this tactile feedback, a 2.5 mm thickness (mean value between the first and the second specimen) was selected.

### 3.3. Three-dimensional printing and assembly of the phantom

The uterus' body and the three cervices were manufactured using a Formlabs Form 3B printer. Four flanges (one for each cervix and one for the body) were made from a Plexiglass panel of thickness 2 mm and shaped using the Adom Vrel Laser CO2-N600/80W laser cutter. Each cervix and body were glued to their respective flange with Super Attack Power Flex Gel from Loctite® and connected using M2.5 bolt coupling to obtain interchangeable disassemblable models. Figure 4 shows the obtained 3D-printed modular phantom.

For convenience, the reclinable support was manufactured using two AM technologies. Some parts were 3D-printed using an Ultimaker 3 and the white Ultimaker Tough PLA (polylactic acid); for the remaining ones, the Form 3B printer and the Formlabs Clear resin were used. The support allows positioning the phantom into the three selected orientations, as shown in Figure 5.

### 3.4 Testing protocol and setup for the evaluation of the intraluminal pressure

To validate the phantom, tests were performed using the Bakri post-partum balloon (Cook Medical, 2021) to demonstrate that the phantom allows the measurement of both ILP and IUP and can be used to validate UBT/CBT devices. The tests for the ILP were performed using the Bakri device inside the phantom, and the results were compared with those measured inside a commercial simulator. The aim was to validate the correct functioning of the modular phantom and to emphasise its advantages over commercial simulators that are not conceived for this purpose.

The Bakri is a disposable device, therefore, not designed to be used several times. However, the ILP and IUP measurements were carried out with the same balloon to

**Figure 4** Modular phantom of the uterus with interchangeable cervices
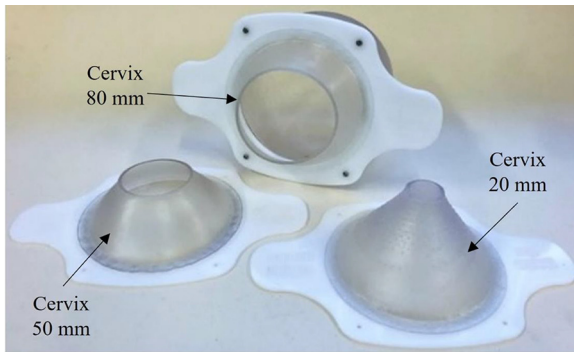


optimise the number of devices needed for the experimental campaign. To this aim, a preconditioning process was applied to the balloon, through inflation/deflation cycles until its stabilisation. Five preconditioning cycles were performed. By gradually filling the Bakri balloon with water up to 500 ml as prescribed in the Instruction of Use, the ILP was measured first without inserting the device in the simulator (i.e. in the air), then by inserting it inside the commercial simulator *Prompt Flex PPH Module* LIM-80101 (Limbs and Things, 2021) which has a 50 mm cervix and, finally, inside the phantom. The ILP was

measured with a pressure transducer (42PC15D pressure sensors, Honeywell Inc.®, Freeport, IL, the USA).

Figure 6 shows the testing setup used to measure the ILP: the Bakri in the air [Figure 6(a)]; the Bakri inserted inside the commercial simulator [Figure 6(b)]; and the Bakri in the modular phantom with two different cervices [Figure 6(c) and 6(d)]. Each measurement was repeated three times. The circuit includes a transducer connected to the internal lumen of the Bakri. The connection is made using two stopcocks: a two-way valve allows opening/closing the hydraulic circuit, while a three-way valve connects the Bakri alternately to the syringe or the transducer for filling/emptying the balloon and measuring the pressure, respectively. A 60 ml syringe was used to fill the balloon gradually and manually. Tests were performed by filling the Bakri progressively with water from 0 to 50 ml using 10 ml and 50 ml steps to reach 500 ml. The pressure developed inside the balloon was measured at each step. The average pressure and the related standard deviation for any given volume were calculated. The measured ILP values for each step were collected through the NI USB-6218 DAQ board (National Instruments, Austin, USA) using LabVIEW software.

For the commercial simulator, support clamps were used [Figure 6(b)] to simulate the physiological inclination of the uterus during childbirth which corresponds to the most

**Figure 5** The phantom, with its reclinable support, in three different inclinations: (a) 100°, (b) 90° and (c) 80°
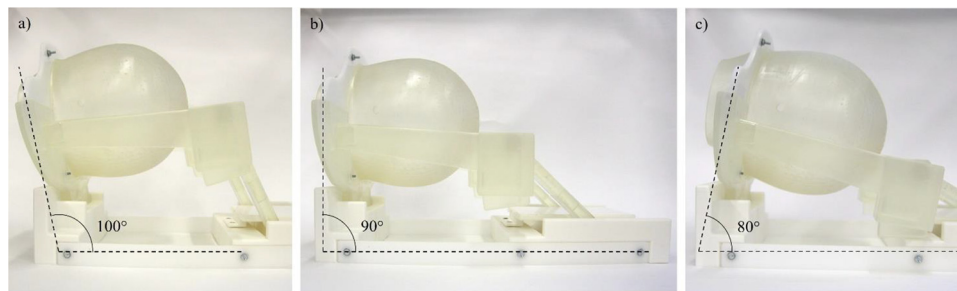


**Figure 6** The setup used for all tests to calculate the intraluminar pressure: (a) Bakri in the air; (b) Bakri inside the commercial simulator; (c) Bakri inside the phantom with the 50 mm cervix; (d) Bakri inside the phantom with the 20 mm cervix
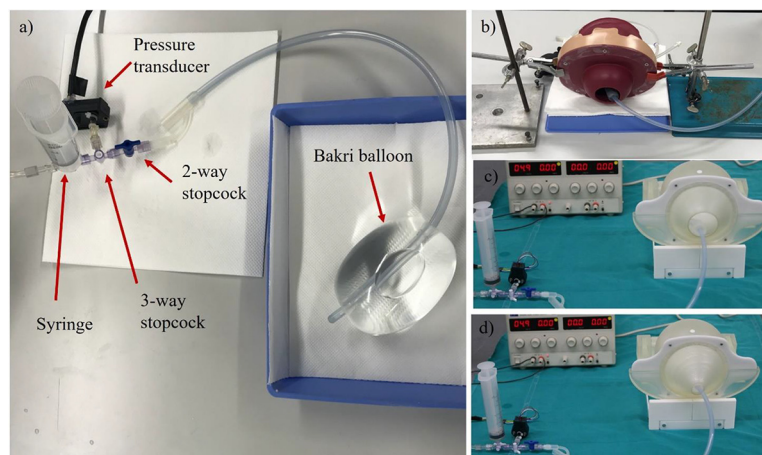
critical inclination for a UBT device. If not correctly supported by the operator, the device can escape from the cervical opening during inflation because of its increased weight and the force of gravity. The sliding of the device from the uterine cavity may compromise the success of tamponade and slow down the whole procedure of contrasting the haemorrhage. Clamps are needed to ensure that the simulator is set at a height equal to that of the phantom and to avoid the influence of height on the pressure measurements. Besides, the Bakri was placed inside the simulator so that the posterior end of the balloon was in line with the cervical opening and did not leak out. Manually, the operator holds the device in line with the cervical opening of the simulator, mimicking what would happen when using the device in a real-life situation.

### 3.5 Testing protocol and setup for the measurement of the intrauterine pressure

The phantom also allowed the measurement of the IUP exerted by the balloon. This pressure was calculated using a 1 psi transducer (42PC1D pressure sensors, Honeywell Inc.®, Freeport, IL, USA) inserted into the rear hole of the uterus body (Figure 7). The transducer was connected to the phantom through a flexible connector to measure the pressure exerted by the balloon on the internal walls of the uterine cavity.

The pressure increases as soon as the balloon, thanks to the inflating, blocks the cervical opening and does not allow air to escape. Therefore, the air inside the uterine cavity compresses and exerts a certain pressure on the internal walls of the phantom. During *in-vivo* conditions, the device cannot exercise the necessary pressure to stop the bleeding directly on the inner walls of the cavity only by contact. The device counteracts the haemorrhage by occluding the cervical opening and exerting a certain pressure on some vascular structures subjected to bleeding because the size of the uterus is bigger than that of the balloon in the maximum inflation condition.

For the IUP measurement, the Bakri was placed inside the cervical opening of the phantom and held manually for the entire test duration to ensure that the posterior limit of the device remained in line with the cervical opening. The balloon was inflated to approximately 500 ml, as previously described for the ILP tests.

Trials were performed with the different configurations of the phantom: in the configuration with the small cervix (20 mm) and the medium cervix (50 mm), pressure begins to develop within the uterine cavity after device inflation when it perfectly occludes the cervical opening. Tests were also performed with the 80 mm cervix configuration. Still, in that case, it was difficult to measure the IUP because the device, even at its maximum inflation, cannot occlude the cervical opening. During PPH treatment, the surgeon proceeds by applying complementary techniques, such as tamponing or using surgical clamps to close the dilatation manually during such a wide dilatation. These approaches facilitate the work of the surgeon and the device under "extreme" conditions. In our case, therefore, it was considered sufficient to test the phantom with the medium and small configurations. For each arrangement, three repetitions were performed to calculate the mean and standard deviation.

## 4. Results and discussion

The preconditioning of the balloon consisted of five inflation/deflating cycles, which led to the five curves shown in Figure 8. In the *first cycle* (Figure 8), the Bakri balloon reached a high initial pressure of 100 mmHg at 50 ml. By repeating these cycles, the pressure values gradually decrease, becoming more homogeneous and reaching a maximum of about 110 mmHg upon reaching 500 ml. The data collected from these first tests made it possible to understand that balloon preconditioning was necessary to avoid any influence on the ILP and IUP values.

After the preconditioning phase, the ILP tests were performed. The interpolated mean curves, with standard deviation, are shown in Figure 9. The tests labelled Bakri in the air reported an average maximum pressure value of 93 mmHg at a filling volume equal to 500 ml, lower than 110 mmHg achieved in the first trial during the preconditioning (*first cycle*, Figure 8). This aspect highlights how the Bakri device is disposable and how its behaviour is affected by the number of inflation/deflation cycles and the amount of water introduced into it. The coefficients of

**Figure 7** Experimental setup for the measurement of the intrauterine pressure
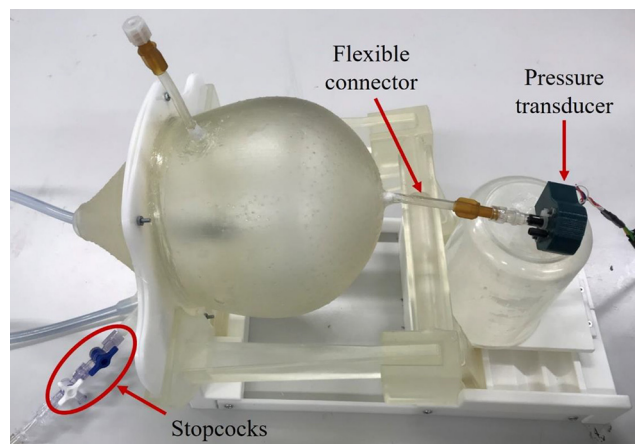
**Figure 8** Preconditioning phase
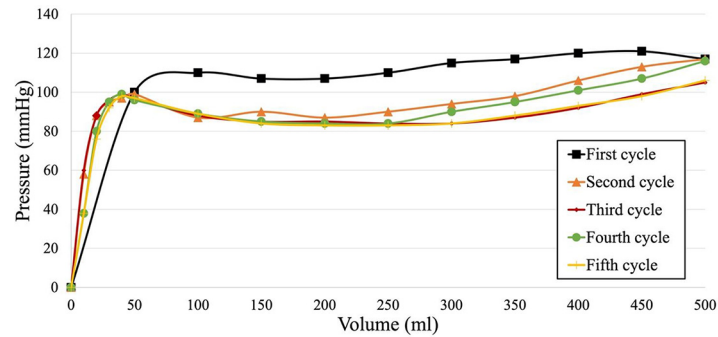


**Figure 9** Average intraluminal pressure with the relative standard deviation developed by the Bakri device in different setups
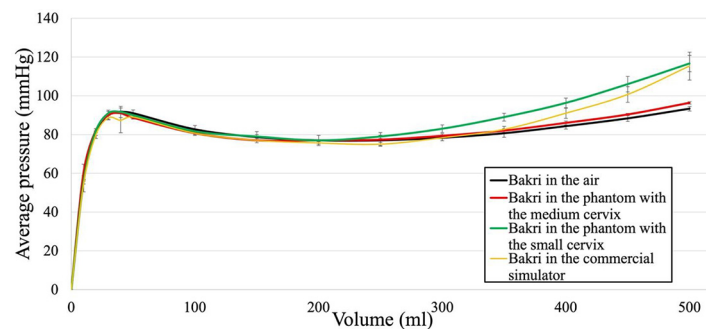


variation were calculated for all the points of the *Bakri in the air* curve: all of them are lower than 0.05, proving that the preconditioning phase was effective and that the three repetitions of this test are comparable.

The second test series was performed using the commercial simulator. In these tests (*Bakri in the commercial simulator*, Figure 9), the mean pressure values are equivalent to those obtained in the previous test (*Bakri in the air*) at low volume values (lower than 350 ml). In comparison, they are higher at high volumes (higher than 350 ml), reaching a maximum value equal to 115 mmHg at 500 ml. This behaviour is because, during the filling, the balloon progressively gets in touch with the internal walls of the simulator, which, counteracting the expansion of the balloon, determines an increase in the ILP value. Also, in this case, the coefficients of variation were computed: they are all lower than 0.05, except for three points (0.08, 0.07 and 0.06 corresponding to filling volumes equal to 10, 40 and 500 ml, respectively). For the two low volumes (i.e. 10 and 40 ml), this higher variability can be because of errors during testing, while for the maximum volume (500 ml), it could be because these tests are operator-dependent.

The third test series was performed using the phantom with the medium cervix (*Bakri in the phantom with the medium cervix*, Figure 9). As in the commercial simulator, the ILP mean values are superimposed to those obtained in the air at low volumes, while they become higher at high filling volumes, reaching a maximum of 96 mmHg at 500 ml. Eventually, the last tests were performed using the phantom with the small cervix. In this case (*Bakri in the phantom with the small cervix*, Figure 9),

the mean pressure values start to deviate from the reference in the air (*Bakri in the air*) at a volume equal to 200 ml, increasing up to a value equal to 117 mmHg at 500 ml. The behaviours of these two last curves are because the Flexible 80 A resin, with a thickness of 2.5 mm, is more deformable than the commercial simulator's material. Hence, comparing the *Bakri in the commercial simulator* curve with the *Bakri in the phantom with the medium cervix* curve, the latter shows a behaviour closer to the *Bakri in the air* curve (Figure 9), as the phantom walls less limit the balloon expansion. The high ILP values of the *Bakri in the phantom with the small cervix* curve are instead because of the geometry of the small cervix. As shown in Figure 4, this cervix has a funnel shape, limiting balloon inflation compared to all other geometries. Also, for these two-test series, the coefficients of variation were lower than 0.05, confirming the repeatability of the tests.

The results of these tests can be read in two ways. On the one hand, they demonstrate the effectiveness of the phantom in allowing the measurement of the ILP needed for the approval of the device. On the other hand, they highlight the dependence of this parameter on multiple factors. From an engineering perspective, it is evident that the ILP value depends on the stiffness of the material the balloon is made of and the environment in which it inflates. In the case of confined expansion, the volume of the uterine cavity and the properties of the material play a crucial role. The commercial simulator and the phantom have an internal volume equal to 650 ml and 2.5 l, respectively. Although the phantom volume is four times bigger than the one of the simulator, comparable ILP curves were obtained because of the different material properties and

the stiffness of the Bakri balloon. This aspect was already highlighted in Antony *et al.* (2017). That study demonstrated that multiple UBT/CBT devices, all effective in obtaining a "positive tamponade" *in-vivo*, are characterised by highly different ILP values, proving that there is not a specific ILP value to be reached. This result underlines another aspect not addressed by other researchers: the extreme need for proper training on using UBT/CBT devices. The tamponade is not guaranteed only by the fact that a device is approved because it can reach the target pressure value but also by the operator's experience and manual skills. Hence, the designed phantom can be used to validate the device and train operators in multiple working conditions.

Figure 10 shows the curves obtained from the measurement of the IUP. Six tests were performed, three with the 50 mm cervix and three with the 20 mm cervix. The IUP increases only when the device completely occludes the cervical opening, and this happens almost instantaneously in the configuration with the 20 mm cervix. Indeed, the balloon immediately fills up and does not allow the escape of air from the uterine cavity. At the same time, it begins to exert pressure on the internal walls of the uterus, compressing the air inside. The pressure starts to rise until it reaches values close to 23 mmHg.

The instant at which the balloon occludes the cervix depends on how full the device is and how the operator holds the device within the cervical opening. In the case of the 50 mm cervix, the various tests' closure of the cervical opening and the increased intrauterine pressure always occur after at least a 250 ml filling. In this case, the onset of pressure growth varies between tests because of the manual procedure. Indeed, the curves do not overlap, as occurs for the 20 mm cervix. The pressure exerted by the balloon on the internal walls of the uterine cavity is higher in the case of the phantom with the 20 mm cervix. This occurs because the balloon occludes sooner the small cervix, and the air inside the phantom compresses as the device inflates.

This result underlines how the operator's experience and capabilities are fundamental to dealing with such variable working conditions, influencing the device design. Indeed, this test has also highlighted that the balloon becomes effective at different filling volumes according to the working conditions. This is an important insight to underline when training the operators in using it and selecting the urinary drain or saline bag to be included in the kit.

**Figure 10** Intrauterine pressure acquired with a phantom equipped with the 50 mm and 20 mm dilation cervices
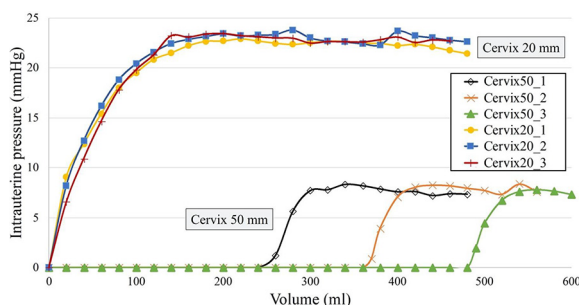


## 5. Conclusions

This paper presents a 3D-printed modular phantom of a uterus for biomedical device validation. This phantom was conceived to test medical devices that counteract PPHs, one of the leading causes of maternal death, especially in LMICs. Although these devices are available, the state-of-the-art analysis has highlighted the lack of a proper setup and procedure to validate their effectiveness and collect design feedback before running *in-vivo* tests, that is, directly on patients.

The contribution of the study is threefold. First, the proposed modular phantom further demonstrates the potential of AM technologies in driving innovation in the medical sector, with a focus on the gynaecological field. The phantom is one of the first examples of a 3D-printed uterus model conceived to validate medical devices. Compared to the model described in Kondoh *et al.* (2019), the proposed phantom is not derived from medical images of a single patient. It is designed using mean dimensional values available in the literature and representing a good compromise between different situations that can occur after the delivery. Moreover, the material and the model's wall thickness were selected to reproduce the real organ's consistency in the best possible way. The multiple commercial uterus simulators nowadays available, such as MamaU, MamaNatalie or the Postpartum Hemorrhage Module – PROMPT Flex (Laerdal, 2021a, 2021b; Limbs and Things, 2021) are conceived for training purposes and not for medical devices validation. For example, they cannot recreate the different moments of childbirth and the natural dilation of the cervix corresponding to caesarean delivery. Instead, the modular architecture of the proposed phantom allows interchanging the cervix having diverse dilations corresponding to distinctive moments of delivery. Unlike the other uterus phantoms, it is possible to simulate both the presence of the vaginal tissue and the condition in which the surgeon manually tampons and reduces the cervical opening. The surgeon performs this tamponing strategy to avoid the leakage of the balloon inserted into the uterus to stop the haemorrhages through the so-called UBT technique. Unlike commercial uterus simulators, the proposed phantom allows testing the device and, thus, collecting design feedback under multiple working conditions. Although the phantom does not include the vaginal tissue, this lack is compensated by the flexibility of the material used to print it. Moreover, it is worth underlying that the phantom (i.e. the uterus plus the three cervixes) can be printed using less than 1 l of material (Flexible 80 A), while the support was 3D-printed using desktop stereolithography and fused filament fabrication machines. Overall, it is an affordable and effective solution that can be fabricated in-house, for example, directly inside hospitals or research labs. Finally, the phantom has been conceived to perform measurements of intraluminal pressure exerted by the balloon, which is necessary to obtain approval from the FDA.

Second, the study details the implemented design process to stimulate the development of more systematic approaches in 3D-printed phantom design. The intent is to further push its diffusion in the medical field for training and surgical planning purposes and as an effective strategy to drive the development of medical devices.

Third, the phantom was 3D-printed using a transparent and flexible material that helps to see the simulation of bleeding inside the model and mimic the uterine tissue's deformability as much as possible. Although its effectiveness was confirmed by the surgeon involved in the study and the performed experimental tests, the study highlights the need for further research to extend the range of AM materials to improve the development of 3D-printed phantom organs specifically conceived to support the design of medical devices. The faithful reproduction reduces the risks of incorrect device design and, consequently, the risks of incorrect device use. AM technologies could, thus, be used to create phantoms capable of supporting the entire validation process of new biomedical devices. It guarantees the measurement of fundamental parameters for validating a UBT device, such as the ILP and the IUP. However, to measure the IUP, the hydraulic seal with the device (an instant that occurs when the inflated device completely occludes the cervical opening) is necessary. If this condition is fulfilled, then the increase in the balloon volume causes the pressure inside the uterine cavity to rise. It, therefore, makes possible the measurement of the IUP at the bottom of the uterus. In the future, it would be interesting to reproduce a condition as similar as possible to the *in-vivo* one, measuring the pressure exerted by the balloon on the walls of the lower uterine segment. This measurement could be performed by inserting in the phantom a force transducer and adding a hole at the level of the cervical walls.

The study's next step is to use the uterus phantom to conduct usability tests of UBT devices involving expert and non-expert operators. These tests could allow to not only further optimise the design of the device in terms of its effectiveness and usability but also push their domestic use, especially in LMICs, in case of difficulties in quickly reaching hospital infrastructures.

# References

Ajao, M.O., Clark, N.V., Kelil, T., Cohen, S.L. and Einarsson, J.I. (2017), "Case report: three-dimensional printed model for deep infiltrating endometriosis", *Journal of Minimally Invasive Gynecology*, Vol. 24 No. 7, pp. 1239-1242.

Antony, K.M., Racusin, D.A., Belfort, M.A. and Dildy, G.A. III (2017), "Under pressure: intraluminal filling pressures of postpartum hemorrhage tamponade balloons", *American Journal of Perinatology Reports*, Vol. 07 No. 2, pp. e86-e92.

ASTM International (2021), *Standard Test Methods for Vulcanized Rubber and Thermoplastic Elastomers-Tension*, ASTM International, West Conshohocken, PA, doi: 10.1520/D0412-16R21.

Bangeas, P., Tsioukas, V., Papadopoulos, V.N. and Tsoulfas, G. (2019), "Role of innovative 3D printing models in the management of hepatobiliary malignancies", *World Journal of Hepatology*, Vol. 11 No. 7, pp. 574-585.

Barbosa, M.Z., Zylbersztejn, D.S., de Mattos, L.A. and Carvalho, L.F. (2019), "Three-dimensionally-printed models in reproductive surgery: systematic review and clinical applications", *Minerva Ginecologica*, Vol. 71 No. 3, pp. 235-244, doi: 10.23736/s0026-4784.19.04319-3.

Bartel, T., Rivard, A., Jimenez, A., Mestres, C.A. and Müller, S. (2018), "Medical three-dimensional printing opens up new opportunities in cardiology and cardiac surgery", *European Heart Journal*, Vol. 39 No. 15, pp. 1246-1254.

Baskaran, V., Štrkalj, G., Štrkalj, M. and Di Ieva, A. (2016), "Current applications and future perspectives of the use of 3D printing in anatomical training and neurosurgery", *Frontiers in Neuroanatomy*, Vol. 10, pp. 1-8.

Belfort, M.A., Dildy, G.A., Garrido, J. and White, G.L. (2011), "Intraluminal pressure in a uterine tamponade balloon is curvilinearly related to the volume of fluid infused", *American Journal of Perinatology*, Vol. 28 No. 8, pp. 659-666.

Candidori, S., De Gaetano, F., Osouli, K., Re, A., Volonté, P., Zanini, A.A., Graziosi, S., Costantino, M.L. (2021), "Fighting maternal bleeding in low-resource settings: an analysis of design and measurement issues", *2021 IEEE International Workshop on Metrology for Industry 4.0 & IoT (MetroInd4.0&IoT)*, pp. 324-329, doi: 10.1109/MetroInd4.0IoT51437.2021.9488502.

Choi, J.W. and Kim, N. (2015), "Clinical application of three-dimensional printing technology in craniofacial plastic surgery", *Archives of Plastic Surgery*, Vol. 42 No. 3, pp. 267-277.

Condous, G.S., Arulkumaran, S., Symonds, I., Chapman, R., Sinha, A. and Razvi, K. (2003), "The 'tamponade test' in the management of massive postpartum hemorrhage", *Obstetrics and Gynecology*, Vol. 101 No. 4, pp. 767-772.

Cook Medical (2021), "Bakri® postpartum balloon with rapid instillation components", available at: www.cookmedical.com/products/wh_sosr_webds/ (accessed 15 January 2022).

Cooke, C., Flaxman, T., Sheikh, A., Althobaity, W., Miguel, O. and Singh, S. (2019), "3D printing in gynecologic surgery – an innovative tool for surgical planning", *Journal of Minimally Invasive Gynecology*, Vol. 26 No. 7, pp. S19-S20.

Danso, D. and Reginald, P.W. (2012), "Internal uterine tamponade", in Arulkumaran, S., Karoshi, M., Keith, L.G., Lalonde, A.B. and B-Lynch, C. (Eds), *A Comprehensive Textbook of Postpartum Hemorrhage. An Essential Clinical Reference for Effective Management*, 2nd ed., Sapiens Publishing, London, pp. 377-380.

DeStephano, C.C., Chou, B., Patel, S., Slattery, R. and Hueppchen, N. (2015), "A randomized controlled trial of birth simulation for medical students", *American Journal of Obstetrics and Gynecology*, Vol. 213 No. 1, pp. 91.e1-91.e7.

Edwards, D.A. and Ellwood, D.A. (2000), "Ultrasonographic evaluation of the postpartum uterus", *Ultrasound in Obstetrics and Gynecology*, Vol. 16 No. 7, pp. 640-643.

Fang, S., McLean, J., Shi, L., Vink, J.S.Y., Hendon, C.P. and Myers, K.M. (2021), "Anisotropic mechanical properties of the human uterus measured by spherical indentation", *Annals of Biomedical Engineering*, Vol. 49 No. 8, pp. 1923-1942.

Flaxman, T.E., Cooke, C.M., Miguel, O.X., Sheikh, A.M. and Singh, S.S. (2021), "A review and guide to creating patient specific 3D printed anatomical models from MRI for benign gynecologic surgery", *3D Printing in Medicine*, Vol. 7 No. 1, pp. 1-10, doi: 10.1186/s41205-021-00107-7.

Food and Drug Administration (2019), "510 (k) clearance for ESM-UBT", available at: www.accessdata.fda.gov/cdrh_docs/pdf19/K191264.pdf (accessed 15 January 2022).

Food and Drug Administration (2021), "Medical devices", available at: www.fda.gov/medical-devices (accessed 15 January 2022).

Formlabs Inc. (2017), "Material data sheet: flexible resin for ergonomic features", available at: https://formlabs-media.formlabs.com/datasheets/Flexible_Technical.pdf (accessed 15 January 2022).

Garg, B. and Mehta, N. (2018), "Current status of 3D printing in spine surgery", *Journal of Clinical Orthopaedics and Trauma*, Vol. 9 No. 3, pp. 218-225.

Gebhardt, A. (2012), *Understanding Additive Manufacturing Rapid Prototyping – Rapid Tooling – Rapid Manufacturing*, Hanser Publishers, Munich, doi: 10.3139/9783446431621.

Georgiou, C. (2010), "Intraluminal pressure readings during the establishment of a positive 'tamponade test' in the management of postpartum haemorrhage", *BJOG: An International Journal of Obstetrics & Gynaecology*, Vol. 117 No. 3, pp. 295-303.

Georgiou, C. (2012), "Intraluminal pressure readings whilst achieving a positive 'tamponade test' in the management of postpartum hemorrhage", in Arulkumaran, S., Karoshi, M., Keith, L.G., Lalonde, A.B. and B-Lynch, C. (Eds), *A Comprehensive Textbook of Postpartum Hemorrhage. An Essential Clinical Reference for Effective Management*, 2nd ed., Sapiens Publishing, London, pp. 369-376.

Ghai, S., Sharma, Y., Jain, N., Satpathy, M. and Pillai, A.K. (2018), "Use of 3-D printing technologies in craniomaxillofacial surgery: a review", *Oral and Maxillofacial Surgery, Oral and Maxillofacial Surgery*, Vol. 22 No. 3, pp. 249-259.

Ghazi, A.E. and Teplitz, B.A. (2020), "Role of 3D printing in surgical education for robotic urology procedures", *Translational Andrology and Urology*, Vol. 9 No. 2, pp. 931-941.

Giannopoulos, A.A., Mitsouras, D., Yoo, S.J., Liu, P.P., Chatzizisis, Y.S. and Rybicki, F.J. (2016), "Applications of 3D printing in cardiovascular diseases", *Nature Reviews Cardiology*, Vol. 13 No. 12, pp. 701-718.

Giannopoulos, A.A., Steigner, M.L., George, E., Barile, M., Hunsaker, A.R., Rybicki, F.J. and Mitsouras, D. (2016), "Cardiothoracic applications of 3-dimensional printing", *Journal of Thoracic Imaging*, Vol. 31 No. 5, pp. 253-272.

Goldstuck, N. (2012), "Assessment of uterine cavity size and shape: a systematic review addressing relevance to intrauterine procedures and events", *African Journal of Reproductive Health*, Vol. 16 No. 3, pp. 130-139.

Hu, K., Lapinski, M.M., Mischler, G., Allen, R.H., Manbachi, A. and Seay, R.C. (2020), "Improved treatment of postpartum hemorrhage: design, development, and bench-top validation of a reusable intrauterine tamponade device for low-resource settings", *Journal of Medical Devices*, Vol. 14 No. 1, pp. 1-7, doi: 10.1115/1.4045965.

Kauer, M., Vuskovic, V., Dual, J., Szekely, G. and Bajka, M. (2002), "Inverse finite element characterization of soft tissues", *Medical Image Analysis*, Vol. 6 No. 3, pp. 275-287.

Kim, M.S., Hansgen, A.R., Wink, O., Quaife, R.A. and Carroll, J.D. (2008), "Rapid prototyping: a new tool in understanding and treating structural heart disease", *Circulation*, Vol. 117 No. 18, pp. 2388-2394.

Kondoh, E., Chigusa, Y., Ueda, A., Mogami, H. and Mandai, M. (2019), "Novel intrauterine balloon tamponade systems for postpartum hemorrhage", *Acta Obstetricia et Gynecologica Scandinavica*, Vol. 98 No. 12, pp. 1612-1617.

Kong, C.W. and To, W.W.K. (2018), "Intraluminal pressure of uterine balloon tamponade in the management of severe postpartum hemorrhage", *Journal of Obstetrics and Gynaecology Research*, Vol. 44 No. 5, pp. 914-921.

Laerdal (2021a), "MamaNatalie birthing simulator", available at: https://laerdal.com/us/products/simulation-training/obstetrics-pediatrics/mamanatalie/ (accessed 15 January 2022).

Laerdal (2021b), "Mama U – postpartum uterus trainer", available at: https://shop.laerdalglobalhealth.com/product/mama-u/ (accessed 28 June 2022).

Limbs and Things (2021), "Postpartum hemorrhage module – PROMPT flex", available at: https://limbsandthings.com/global/products/80101/80101-postpartum-hemorrhage-module-prompt-flex (accessed 15 January 2022).

Louwagie, E.M., Carlson, L., Over, V., Mao, L., Fang, S., Westervelt, A., Vink, J., Hall, T., Feltovich, H. and Myers, K. (2021), "Longitudinal ultrasonic dimensions and parametric solid models of the gravid uterus and cervix", *Plos One*, Vol. 16 No. 1, pp. 1-20.

Mackey, A., Ng, J.I., Core, J., Nguyen, L., Cross, D., Lim, P., Woodfield, C., Pugliese, R. and Ku, B. (2019), "Three-dimensional-printed uterine model for surgical planning of a cesarean delivery complicated by multiple myomas", *Obstetrics & Gynecology*, Vol. 133 No. 4, pp. 720-724.

Marconi, S., Pugliese, L., Botti, M., Peri, A., Cavazzi, E., Latteri, S., Auricchio, F. and Pietrabissa, A. (2017), "Value of 3D printing for the comprehension of surgical anatomy", *Surgical Endoscopy*, Vol. 31 No. 10, pp. 4102-4110.

Marone, E.M., Rinaldi, L.F., Pietrabissa, A. and Argenteri, A. (2018), "Effectiveness of 3d printed models in obtaining informed consent to complex aortic surgery", *The Journal of Cardiovascular Surgery*, Vol. 59 No. 3, pp. 488-489.

Massachusetts General Hospital (2021), "Every second matters for mothers and babies: uterine balloon tamponade for postpartum hemorrhage", available at: www.massgeneral.org/emergency-medicine/global-health/initiatives-and-programs/every-second-matters-for-mothers-and-babies-uterine-balloon-tamponade-for-postpartum-hemorrhage (accessed 15 January 2022).

Mathews, D.A.P., Baird, A. and Lucky, M. (2020), "Innovation in urology: three dimensional printing and its clinical application", *Frontiers in Surgery*, Vol. 7, pp. 1-13.

Mazza, E., Nava, A., Bauer, M., Winter, R., Bajka, M. and Holzapfel, G.A. (2006), "Mechanical properties of the human uterine cervix: an in vivo study", *Medical Image Analysis*, Vol. 10 No. 2, pp. 125-136.

MedicalAidFilms (2021), "MedicalAidFilms", available at: www.medicalaidfilms.org/film/uterine-balloon-tamponade/ (accessed 15 January 2022).

Meglioli, M., Naveau, A., Macaluso, G.M. and Catros, S. (2020), "3D printed bone models in oral and cranio-maxillofacial surgery: a systematic review", *3D Printing in Medicine*, Vol. 6 No. 1, pp. 1-18, doi: 10.1186/s41205-020-00082-5.

Mishra, N., Agrawal, S., Gulabani, K. and Shrivastava, C. (2016), "Use of an innovative condom balloon tamponade in

postpartum haemorrhage: a report", *The Journal of Obstetrics and Gynecology of India*, Vol. 66 No. 1, pp. 63-67.

Mollazadeh-Moghaddam, K., Dundek, M., Bellare, A., Borovac-Pinheiro, A., Won, A. and Burke, T.F. (2019), "Mechanical properties of the every second matters for mothers-uterine balloon tamponade (ESM-UBT) device: in vitro tests", *American Journal of Perinatology Reports*, Vol. 09 No. 4, pp. E376-E383.

Muguruza Blanco, A., Krauel, L. and Fenollosa Artés, F. (2019), "Development of a patients-specific 3D-printed preoperative planning and training tool, with functionalized internal surfaces, for complex oncologic cases", *Rapid Prototyping Journal*, Vol. 25 No. 2, pp. 363-377.

Myers, K.M., Paskaleva, A.P., House, M. and Socrate, S. (2008), "Mechanical and biochemical properties of human cervical tissue", *Acta Biomaterialia*, Vol. 4 No. 1, pp. 104-116.

Myers, K.M., Socrate, S., Paskaleva, A. and House, M. (2010), "A study of the anisotropy and tension/compression behavior of human cervical tissue", *Journal of Biomechanical Engineering*, Vol. 132 No. 2, pp. 1-15.

Paliulyte, V., Drasutiene, G.S., Ramasauskaite, D., Bartkeviciene, D., Zakareviciene, J. and Kurmanavicius, J. (2017), "Physiological uterine involution in primiparous and multiparous women: ultrasound study", *Obstetrics and Gynecology International*, Vol. 2017, Article ID 6739345, pp. 1-10, doi: 10.1155/2017/6739345.

Perica, E.R. and Sun, Z. (2018), "A systematic review of Three-Dimensional printing in liver disease", *Journal of Digital Imaging*, Vol. 31 No. 5, pp. 692-701.

Pietrabissa, A., Marconi, S., Negrello, E., Mauri, V., Peri, A., Pugliese, L., Marone, E.M. and Auricchio, F. (2020), "An overview on 3D printing for abdominal surgery", *Surgical Endoscopy*, Vol. 34 No. 1, pp. 1-13.

Randazzo, M., Pisapia, J., Singh, N. and Thawani, J. (2016), "3D printing in neurosurgery: a systematic review", *Surgical Neurology International*, Vol. 7 No. 33, pp. S801-S809.

Riedle, H., Ghazy, A., Seufert, A., Seitz, V., Dorweiler, B. and Franke, J. (2021), "Generic design of an anatomical heart model optimized for additive manufacturing with silicone", *Rapid Prototyping Journal*, Vol. 27 No. 2, pp. 217-222.

Sayed Aluwee, S.B., Zhou, X., Kato, H., Makino, H., Muramatsu, C., Hara, T., Matsuo, M. and Fujita, H. (2017), "Evaluation of pre-surgical models for uterine surgery by use of three-dimensional printing and mold casting", *Radiological Physics and Technology*, Vol. 10 No. 3, pp. 279-285.

Senkoylu, A., Daldal, I. and Cetinkaya, M. (2020), "3D printing and spine surgery", *Journal of Orthopaedic Surgery*, Vol. 28 No. 2, pp. 1-7.

Sheha, E.D., Gandhi, S.D. and Colman, M.W. (2019), "3D printing in spine surgery", *Annals of Translational Medicine*, Vol. 7 No. S5, p. S164.

Smelt, J.L.C., Suri, T., Valencia, O., Jahangiri, M., Rhode, K., Nair, A. and Bille, A. (2019), "Operative planning in thoracic surgery: a pilot study comparing imaging techniques and three-dimensional printing", *The Annals of Thoracic Surgery*, Vol. 107 No. 2, pp. 401-406.

Soon, D.S.C., Chae, M.P., Pilgrim, C.H.C., Rozen, W.M., Spychal, R.T. and Hunter-Smith, D.J. (2016), "3D haptic modelling for preoperative planning of hepatic resection: a systematic review", *Annals of Medicine and Surgery*, Vol. 10, pp. 1-7, doi: 10.1016/j.amsu.2016.07.002.

Sun, Z. (2020), "Patient-Specific 3D printing in liver disease", in Radu-Ionita, F., Pyrsopoulos, N.T., Jinga, M., Tintoiu, I.C., Sun, Z. and Bontas, E. (Eds), *Liver Diseases*, Springer, pp. 493-501.

Tejo-Otero, A., Buj-Corral, I. and Fenollosa-Artés, F. (2020a), "3D printing in medicine for preoperative surgical planning: a review", *Annals of Biomedical Engineering*, Vol. 48 No. 2, pp. 536-555.

Tejo-Otero, A., Colly, A., Courtial, E.J., Fenollosa-Artés, F., Buj-Corral, I. and A. Marquette, C. (2021), "Soft-tissue-mimicking using silicones for the manufacturing of soft phantoms by fresh 3D printing", *Rapid Prototyping Journal*, Vol. 28 No. 2, pp. 285-296, doi: 10.1108/RPJ-04-2021-0079.

Tejo-Otero, A., Fenollosa-Artés, F., Achaerandio, I., Rey-Vinolas, S., Buj-Corral, I., Mateos-Timoneda, M.Á. and Engel, E. (2022), "Soft-tissue-mimicking using hydrogels for the development of phantoms", *Gels*, Vol. 8 No. 1, pp. 1-14.

Tejo-Otero, A., Lustig-Gainza, P., Fenollosa-Artés, F., Valls, A., Krauel, L. and Buj-Corral, I. (2020b), "3D printed soft surgical planning prototype for a biliary tract rhabdomyosarcoma", *Journal of the Mechanical Behavior of Biomedical Materials*, Vol. 109, pp. 1-11.

United Nations (2021), "UN sustainable development goals", available at: www.un.org/sustainabledevelopment/ (accessed 15 January 2022).

Vakharia, V.N., Vakharia, N.N. and Hill, C.S. (2016), "Review of 3-Dimensional printing on cranial neurosurgery simulation training", *World Neurosurgery*, Vol. 88, pp. 188-198.

Vukicevic, M., Mosadegh, B., Min, J.K. and Little, S.H. (2017), "Cardiac 3D printing and its future directions", *JACC: Cardiovascular Imaging*, Vol. 10 No. 2, pp. 171-184.

Wang, L., Ye, X., Hao, Q., Chen, Y., Chen, X., Wang, H., Wang, R., Zhao, Y. and Zhao, J. (2017), "Comparison of two three-dimensional printed models of complex intracranial aneurysms for surgical simulation", *World Neurosurgery*, Vol. 103, pp. 671-679.

Whalen, M., Chang-Davidson, E., Moran, T., Hoffman, R., Frydman, G.H., Slocum, A. and Dangel, A. (2021), "Device prototype for vaginal delivery of extremely preterm fetuses in the breech presentation", *Journal of Medical Devices*, Vol. 15 No. 2, pp. 1-7.

Wilcox, B., Mobbs, R.J., Wu, A.-M. and Phan, K. (2017), "Systematic review of 3D printing in spinal surgery: the current state of play", *Journal of Spine Surgery*, Vol. 3 No. 3, pp. 433-443.

Witowski, J.S., Coles-Black, J., Zuzak, T.Z., Pe̜dziwiatr, M., Chuen, J., Major, P. and Budzyński, A. (2017), "3D printing in liver surgery: a systematic review", *Telemedicine and e-Health*, Vol. 23 No. 12, pp. 943-947.

World Health Organization (2012), "WHO recommendations for the prevention and treatment of postpartum haemorrhage, world health organization, Geneva", available at: www.who.int/publications/i/item/9789241548502

Yap, Y.L., Tan, Y.S.E., Tan, H.K.J., Peh, Z.K., Low, X.Y., Yeong, W.Y., Tan, C.S.H. and Laude, A. (2017), "3D printed bio-models for medical applications", *Rapid Prototyping Journal*, Vol. 23 No. 2, pp. 227-235.

Yoo, S.J. and van Arsdell, G.S. (2018), "3D printing in surgical management of double outlet right ventricle", *Frontiers in Pediatrics*, Vol. 5, No. 289, pp. 1-6, doi: 10.3389/fped.2017.00289.

Yoo, S.-J., Thabit, O., Kim, E.K., Ide, H., Yim, D., Dragulescu, A., Seed, M., Grosse-Wortmann, L. and van Arsdell, G. (2016), "3D printing in medicine of congenital heart diseases", *3D Printing in Medicine*, Vol. 2 No. 3, pp. 1-12, doi: 10.1186/s41205-016-0004-x.

## Corresponding author

**Serena Graziosi** can be contacted at: serena.graziosi@polimi.it